LA-10566-MS

Los Alamos National Laboratory is operated by the University of California for the United States Department of Energy under contract W-7405-ENG-36.

...nglish Striations and the ...Kelvin-Helmholtz Instability: Part I

Los Alamos National Laboratory
Los Alamos, New Mexico 87545

LA-10566-MS

UC-34
Issued: October 1985

Kingfish Striations and the Kelvin-Helmholtz Instability: Part 1

James H. Hunter, Jr.*

*Collaborator at Los Alamos. Department of Astronomy, University of Florida, Gainesville, FL 32611.

Los Alamos National Laboratory
Los Alamos, New Mexico 87545

KINGFISH STRIATIONS AND THE KELVIN-HELMHOLTZ INSTABILITY: PART 1

by

James H. Hunter, Jr.

ABSTRACT

The role of the Kelvin-Helmholtz instability in initiating the formation of the density striations observed in the Kingfish fireball is examined. Two idealized models are proposed for the velocity shear layer on the sides of the fireball, each of which includes essential characteristics of the Kingfish event insofar as the development of Kelvin-Helmholtz instabilities is concerned. A complete linear analysis is presented for each model.

I. INTRODUCTION

The photographic records of the Kingfish fireball reveal the presence of regularly spaced striations aligned along the magnetic fields on the surface of the fireball. The striations appear first, and grow most rapidly, on the sides of the fireball. They appear dramatically at a well-established time after the detonation. The approximate e-folding time for the instability is known.

Detailed numerical simulations of the rising Kingfish fireball show that, when the striations appear, positive ions (principally O^+) outside the fireball, but behind the shock, would be rigidly attached to the magnetic field and therefore would slip past the regions on the fireball where the striations are observed. Essentially, the slip speed would be that of the rising fireball, U. Moreover, estimates show that the resulting shear layer would be thin, having a thickness considerably less than the separation between adjacent striations. The velocity shear and slip velocity would be greatest on the sides of the fireball where the striations first appear. This suggests that the striations may be caused (i.e., initiated) by a Kelvin-Helmholtz instability. On morphological grounds, a Rayleigh-Taylor instability seems

less likely because that instability would be expected to grow most rapidly on the top of the fireball where the fluid deceleration is greatest.

Our purpose in this report is to review selected aspects of linear Kelvin-Helmholtz instability theory in the context of the Kingfish event. In Section II, we formulate an idealized problem, which retains the essential ingredients of the Kingfish event insofar as the development of Kelvin-Helmholtz instabilities is concerned. In Sections III and IV, we consider carefully two models, each of which can be analyzed in a straightforward fashion without resorting to extensive numerical calculations. Although idealized, each of these models has a direct bearing on the problem at hand.

II. FORMULATION OF THE PROBLEM

In this section, we consider the Kelvin-Helmholtz instability (hereafter, designated K-H instability) in a compressible, magnetized fluid. The ideal MHD equations are

$$\frac{d\rho}{dt} = -\underset{\sim}{\nabla} \cdot \rho \underset{\sim}{V} \ , \tag{1}$$

$$\rho \frac{d\underset{\sim}{V}}{dt} = -\underset{\sim}{\nabla}\left(p + \frac{B^2}{8\pi}\right) + \frac{1}{4\pi} (\underset{\sim}{B} \cdot \underset{\sim}{\nabla})\underset{\sim}{B} + \underset{\sim}{f} \ , \tag{2}$$

$$\frac{\partial \underset{\sim}{B}}{\partial t} = \underset{\sim}{\nabla} \times (\underset{\sim}{V} \times \underset{\sim}{B}) \ , \tag{3}$$

and

$$\frac{dp}{dt} = \frac{\gamma_g p}{\rho} \frac{d\rho}{dt} \ , \tag{4}$$

where ρ is the density, $\underset{\sim}{V}$ the bulk velocity, $\underset{\sim}{B}$ the magnetic field strength, P the fluid pressure, and γ_g the adiabatic index. The $\underset{\sim}{f}$ vector represents additional body forces per unit mass, and the convective derivative $d/dt = \partial/\partial t + \underset{\sim}{V} \cdot \underset{\sim}{\nabla}$. Because the observed structures are relatively small

compared with the fireball radius, the linear problem will be formulated in Cartesian coordinates. In the following development, we adopt the conventional notation of Chandrasekhar.[1] The physical situation is illustrated in Fig. 1. In our problem, the undisturbed magnetic field, bulk velocity, and force vectors are given by $\underset{\sim}{B} = \underset{\sim}{j}B$, $\underset{\sim}{U} = \underset{\sim}{i}U(z)$, and $\underset{\sim}{f} = -\underset{\sim}{k}f$, where $\underset{\sim}{i}$, $\underset{\sim}{j}$, and $\underset{\sim}{k}$ are unit vectors in the x, y, and z directions respectively. The equilibrium condition requires that $D(p + B^2/8\pi) = f$, where $D \equiv d/dz$. In formulating the idealized problem, f will be zero, meaning that gradients are allowed only in U(z). Therefore, in a formal sense, unperturbed pressure equilibrium will be imposed; $p + B^2/8\pi = \text{constant}$. In reality, gradients exist in P, B, and ρ, due to the acceleration of the Earth's gravity, and to dynamical forces associated with the rising fireball. Therefore, to apply linear analysis to the Kingfish problem, we will use model results to gain insight into the behaviors of compressible K-H instabilities. In Section III we will examine idealized models in which the undisturbed media are in pressure equilibrium.

The linearization of Equations (1)-(4) is straightforward and has been outlined in some detail by Miura and Pritchett[2] (hereafter, designated by MP). They Fourier analyze the linear, dependent variables. In our notation, this analysis requires that any perturbed quantity $\xi' = \xi'(z)\exp[i(k_1x+k_2y+nt)]$. When $f = 0$, their second-order eigenvalue equation for the total pressure perturbation is $p'^* = p' + \underset{\sim}{B} \cdot \underset{\sim}{B}'/4\pi$, which reduces to

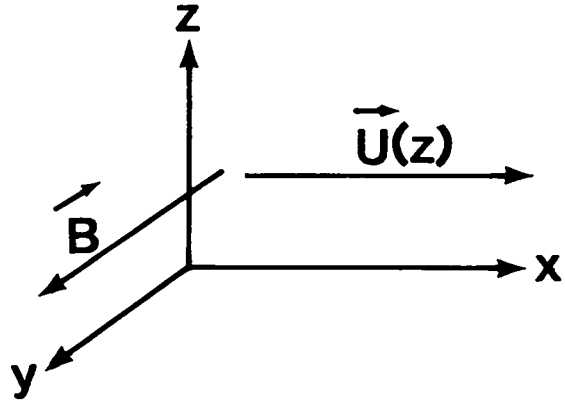

Fig. 1. The coordinate system used in the calculations. Inhomogeneities occur in the z direction only.

$$\phi^2 gD\left(\frac{1}{\phi^2 g} Dp'^*\right) - \left[k_1^2 + k_2^2 - \frac{\phi^2}{(gc^2 + V_A^2)}\right] p'^* = 0 \quad , \tag{5}$$

where $\phi = (n + k_1 U)$ and $g = 1 - k_3^2 V_A^2/\phi^2$. In Equation (5), the Alfvén speed, V_A, and the adiabatic sound speed, c, in the undisturbed medium are defined by $V_A^2 = B^2/(4\pi\rho)$ and $c^2 = \gamma_g p/\rho$. In our problem, the Alfvén speed in the relatively tenuous, slipping medium is much greater than either c or U. Consequently, the Mach number, $m = U/\sqrt{V_A^2 + c^2}$, is small, and the gas will behave very nearly like an incompressible fluid. In the incompressible limit, K-H instabilities are suppressed[2] if $U < 2\, V_A(\underset{\sim}{k} \cdot \underset{\sim}{B})/(k_1 B)$. In the present problem, in which $U/V_A << 1$, K-H instabilities can develop only if $\underset{\sim}{k}$ is very nearly orthogonal to $\underset{\sim}{B}$. Therefore, in the following development, we restrict our attention to the most favorable (transverse) class of models in which the wave vectors are directed parallel to the undisturbed flows; $\underset{\sim}{k} = \underset{\sim}{i} k_1$. (We recall that the Kingfish striations, which correspond to density maxima, are aligned parallel to $\underset{\sim}{B}$, an observation which would follow if the transverse case applies.)

In the transverse case the linear equations describing our problem are

$$\phi p'^* = \frac{B}{4\pi} \phi B_y' - k_1 c^2 \rho u' + i c^2 \rho D w' \quad , \tag{6}$$

$$\rho \phi u' = -k_1 p'^* + i\, \rho\, (DU) w' \quad , \tag{7}$$

$$\rho \phi w' = i D p'^* \quad , \tag{8}$$

and

$$\phi B_y' = -k_1 B u' + i B D w' \quad . \tag{9}$$

In these equations, u' and w' are the velocity perturbations in the x and z directions respectively, and $p'^* = p' + (B/4\pi)B_y' = c^2\rho' + (B/4\pi)B_y'$. Equations (6) and (9) may be combined to give the result

$$\phi p'^* = -k_1 V^2 \rho u' + iV^2 \rho D w' \quad , \tag{10}$$

where $V^2 = V_A^2 + c^2$. Equations (7), (8), and (10) describe forms exactly the same as their hydrodynamic counterparts if the sound speed is replaced by V. Thus, the transverse hydromagnetic problem is formally equivalent to a hydrodynamic problem with $\underset{\sim}{k} = \underset{\sim}{i}k_1$. However, the magnetized medium is less compressible due to the presence of magnetic pressure.

We eliminate variables in the above system to obtain eigenvalue equations for both p'^* and w'. The equation for p'^* reads

$$\left[D^2 - \frac{2k_1(DU)D}{\phi} + \frac{\phi^2}{V^2} - k_1^2\right] p'^* = 0 \quad , \tag{11}$$

exactly the MP result when $k_2 = k_3 = 0$. The eigenvalue equation for w' is more difficult to derive; our result is

$$\left\{D^2 - \frac{2\phi k_1(DU)}{(\phi^2 - k_1^2V^2)} D + \left[\frac{\phi^2}{V^2} - k_1^2 - \frac{k_1(D^2U)}{\phi} + \frac{2k_1^2(DU)^2}{(\phi^2 - k_1^2V^2)}\right]\right\} w' = 0 \quad . \tag{12}$$

To recover the incompressible limit, we let $V \to \infty$. In that limit, Equation (12) reduces to

$$\left[\phi(D^2 - k_1^2) - k_1(D^2U)\right] w' = 0 \quad , \tag{13}$$

exactly Chandrasekhar's result[1] for an incompressible fluid in the absence of unperturbed density gradients. It should be noted that Equations (11) and (12) have different forms. Generally speaking, the eigenvalue equations will be different for the various perturbed quantities when gradients are present in the undisturbed medium. If U is constant, Equations (11) and (12) reduce to the identical forms:

$$\left(D^2 - k_1^2 + \frac{\phi^2}{V^2}\right)(p'^*, w') = 0 \quad . \tag{14}$$

III. THE GENERALIZED GERWIN PROBLEM

In a seminal paper, Gerwin[3] considered the development of K-H instabilities at the interface between two compressible isotropic fluids having identical undisturbed densities and pressures, which flow relative to each other at a constant velocity parallel to the interface. In this section, we generalize Gerwin's problem to include cases in which the densities in the media are unequal. The physical problem is illustrated in Fig. 2. We adopt the convention that $\rho_1 < \rho_2$. If the media are in approximate pressure equilibrium, $\rho_1 V_1^2 = \rho_2 V_2^2$.

In each medium, the total pressure perturbation must satisfy Equation (14). Since U is either constant or zero, the ϕ's are constant in both media. Consequently, the solutions of Equation (14) are of the form $\exp\pm(qz)$, where $q^2 - k_1^2 + \phi^2/V^2 = 0$. If $(n + k_1 U)^2/(k_1^2 V_1^2)$ and $n^2/(k_1^2 V_2^2) < 1$, then

$$q_1 = -k_1 \left[1 - \frac{(n + k_1 U)^2}{k_1^2 V_1^2}\right]^{1/2} \quad , \tag{15a}$$

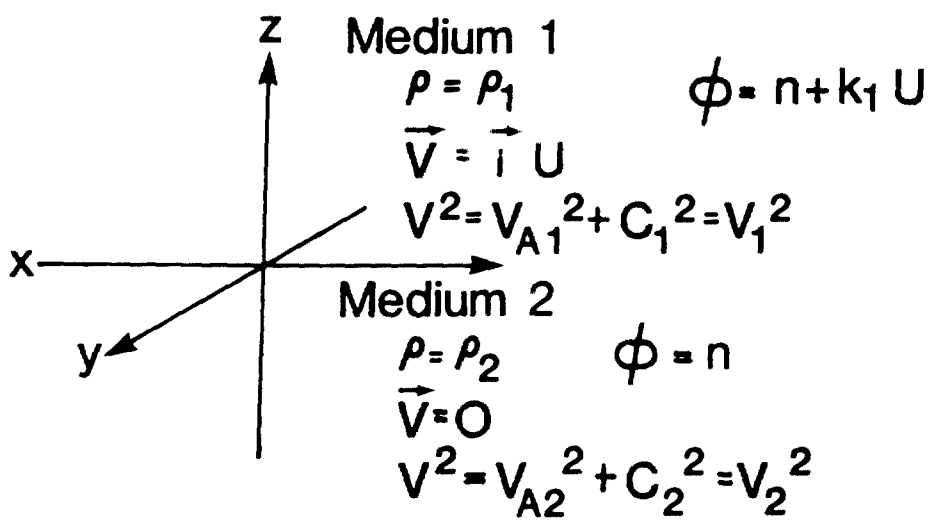

Fig. 2. The generalized Gerwin problem.

and

$$q_2 = \mp k_1 \left(1 - \frac{n^2}{v_2^2}\right)^{1/2} \quad . \tag{15b}$$

The signs associated with $q_{1,2}$ follow from the requirement that the perturbations must vanish as $z \to \pm\infty$. [If $\phi_{1,2}^2/(k_1^2 v_{1,2}^2) > 0$, then the $q_{1,2}$ values will be imaginary. In that event, only outgoing waves can be allowed as $z \to \pm\infty$. Such cases do not concern us in the present application.]

By definition, the linear z velocity, w', and z displacement, z', are related by

$$i \phi z' = w' \quad . \tag{16}$$

Combining Equations (8) and (16), we obtain the expression

$$\rho\phi^2 z' = Dp'^* = qp'^* \quad , \tag{17}$$

a result that holds for both regions 1 and 2. Hence, at the interface of these respective regions, we may write

$$\rho_1 \phi_1^2 z'_{1i} = q_1 p'^*_{1i} \tag{18a}$$

and

$$\rho_2 \phi_2^2 z'_{2i} = q_2 p'^*_{2i} \quad , \tag{18b}$$

where subscript i denotes the interface. At the interface, the continuity conditions are

$$z'_{1i} = z'_{2i} \tag{19a}$$

and

$$p'_{1f} = p'_{2f} \ . \tag{19b}$$

Equations (15a,b), (18a,b), and (19a,b) may be combined, along with the definitions of $\phi_{1,2}$, to yield the desired dispersion relation

$$\frac{\rho_2 n^2}{\left[1 - \frac{n^2}{k_1^2 V_2^2}\right]^{1/2}} = \frac{-\rho_1 (n + k_1 U)^2}{\left[1 - \frac{(n + k_1 U)^2}{(k_1^2 V_1^2)}\right]^{1/2}} \ . \tag{20}$$

We note in passing that the general dispersion relation for the hydrodynamic version of this problem reads

$$\frac{\rho_2 n^2}{\left[1 - \frac{n^2}{(k^2 c_2^2)}\right]^{1/2}} = \frac{-\rho_1 (n + kU\cos\theta)^2}{\left[1 - \frac{(n + kU\cos\theta)^2}{(k^2 c_1^2)}\right]^{1/2}} \ , \tag{21}$$

where θ is the angle between the wave vector $\underset{\sim}{k} = \underset{\sim}{i} k_1 + \underset{\sim}{j} k_2$ and $\underset{\sim}{U}$. Thus, to recover the general hydrodynamic result, we replace $V_{1,2}$ with $c_{1,2}$, k_1 with k, and U with $U\cos\theta$ in Equation (20).

When we define the dimensionless quantities $x = n/(k_1 V_1)$, $a = \rho_1/\rho_2$, $b = (V_1/V_2)^2$, and Mach number $m = U/V_1$, Equation (20) becomes

$$\frac{a(x + m)^2}{\left[1 - (x + m)^2\right]^{1/2}} = \frac{-x^2}{(1 - bx^2)^{1/2}} \ . \tag{22}$$

Equation (22) is of 6th order in x. After squaring both sides, and rearranging terms, we obtain

$$(1 - a^2b)x^6 + 2m(1 - 2a^2b)x^5 + (m^2 - 6a^2bm^2 + a^2 - 1)x^4$$

$$+ 4ma^2(1 - bm^2)x^3 - m^2a^2(bm^2 - 6)x^2 + 4a^2m^3x + a^2m^4 = 0 \quad . \tag{23}$$

Equation (23) has only one complex conjugate pair of roots, which also satisfies Equation (22). These roots, which represent the K-H modes, may be written as $x = x_r \pm ix_i$. The growing mode has the negative sign, and its growth rate is $\gamma = x_i k_1 V_1 = X_i k_1 (U/m)$.

In the incompressible limit (m = 0), the roots of Equation (20) are

$$n = -\alpha k_1 U \pm i \sqrt{\alpha(1 - \alpha)} k_1 U \quad , \tag{24}$$

where $\alpha = \rho_1/(\rho_1 + \rho_2)$. The ratio of oscillatory frequency, ω, to growth rate γ is $\omega/\gamma = (\rho_1/\rho_2)^{1/2}$. The most rapid growth occurs when $\alpha = 1/2$, corresponding to a = 1. In this case, Equation (20) can be expanded easily in powers of m to gauge the influence of compressibility on the growth rates. Thus, we obtain

$$n \simeq - k_1 \frac{U}{2} \pm i \, k_1 \frac{U}{2} \left(1 - \frac{m^2}{4}\right) \quad . \tag{25}$$

It is evident that compressibility reduces the unstable growth rates, which is to be expected on physical grounds. When m = 0.01, the complex growth rate calculated from Equation (25) is identical to the corresponding numerical solution of Equation (23) to nine significant figures; when m = 0.20, the results agree to four significant figures; when m = 1.00, the growth rate predicted by Equation (25) is low by ~7.5%.

The growth rates of the unstable K-H modes are shown in Fig. 3 for Gerwin's case; a = b = 1, where we have defined $n \equiv \pm i\gamma + \omega$. These solutions can be derived analytically because Equation (23) reduces to a quintic, having one root $x_5 = -m/2$. The remaining quartic equation can be solved algebraically. As noted by Gerwin,[3] K-H instabilities can occur only when $m < \sqrt{8}$. As ρ_1/ρ_2 diminishes, the K-H growth rates usually become smaller.

Moreover, unless V_2/V_2 is very large, the range of m values over which these instabilities can arise shrinks as well. This behavior is illustrated in Fig. 4. The curves represent models for which the undisturbed media are constrained by the condition $\rho_1 V_1^2 = \rho_2 V_2^2$. If $V_A^2/c^2 \gg 1$, $c^2/V_A^2 \gg 1$, or $\gamma_g = 2$, this condition amounts to requiring that regions 1 and 2 be in pressure equilibrium. [Strictly speaking, pressure equilibrium requires that $\rho_1(c_1^2/\gamma_g + V_{A1}^2/2) = \rho_2(c_2^2/\gamma_g + V_{A2}^2/2)$.] Cases conforming to the unphysical condition, $\rho_1 V_1 = \rho_2 V_2$, are depicted in Fig. 5. If this condition of "momentum equilibrium" is met, the growth rates remain relatively large as ρ_1/ρ_2 becomes small. In physical terms, the ratio of the "thermal" energy density of the fluid in region 1 to that in region 2 = $V_1/V_2 = \rho_2/\rho_1$. Consequently, ample energy is always available to drive the K-H instabilities. Figure 6 shows the normalized maximum rates (and corresponding Mach numbers) for "pressure equilibrium" models ($\rho_1 V_1^2 = \rho_2 V_2^2$) as a function of density contrast. Clearly, the growth rates of K-H instabilities diminish as the density contrast increases for reasonable physical models. Unlike the case for small m [in which $\omega/\gamma = (\rho_1/\rho_2)^{1/2}$], the ratios of the corresponding oscillatory frequencies to these maximum growth rates are $\omega/\gamma_m \sim 1$.

IV. INCOMPRESSIBLE MODELS WITH LINEAR SHEAR LAYERS

While the models of Section III have the virtue of including compressibility, they suffer from the shortcoming of imposing a velocity discontinuity between regions 1 and 2. Since shear viscosity was not included in these models, the shorter the Fourier wavelength, the more rapid will be the K-H growth rate. However, if K-H instabilities are responsible for the Kingfish striations, the observations show that a preferred wavelength is excited. As is the case when shear viscosity is present, the existence of a finite shear layer in a velocity profile will select a favored wavelength for which the K-H growth rate is a maximum. From a physical viewpoint, shear viscosity and velocity shear are related. If a discontinuous velocity profile is imposed upon a viscous fluid, then subsequently a shear layer will develop in the fluid through the action of shear viscosity. (Indeed, a linear velocity profile can be maintained in the presence of any constant coefficient of shear viscosity.)

For models having uniform, undisturbed densities, both MP[2] and Chandrasekhar[1] have shown that incompressible K-H instabilities experience a

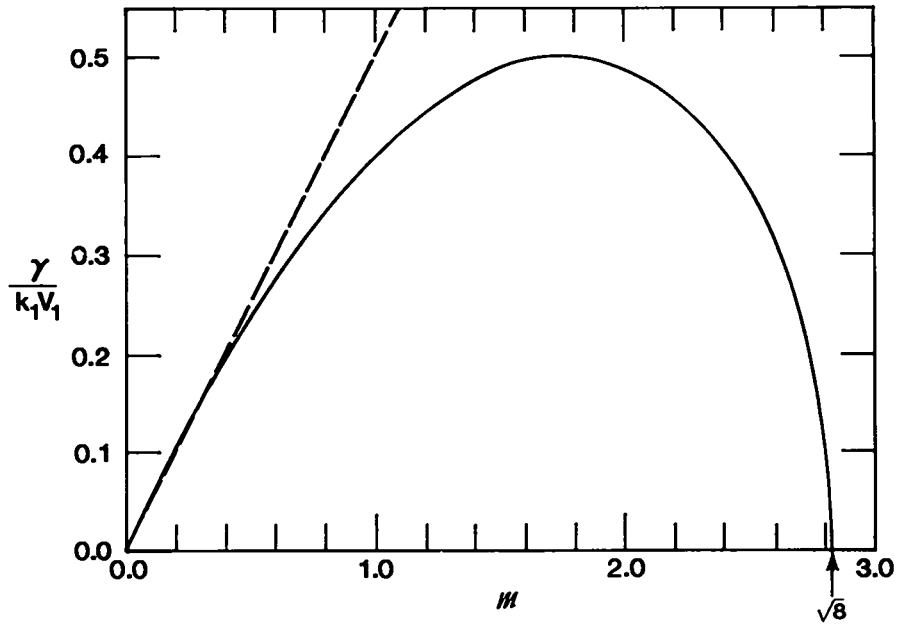

Fig. 3. Unstable growth rates in the Gerwin problem; $\rho_1/\rho_2 = 1$. The dashed line shows the incompressible growth rate, $\gamma/(k_1V_1) = m/2$.

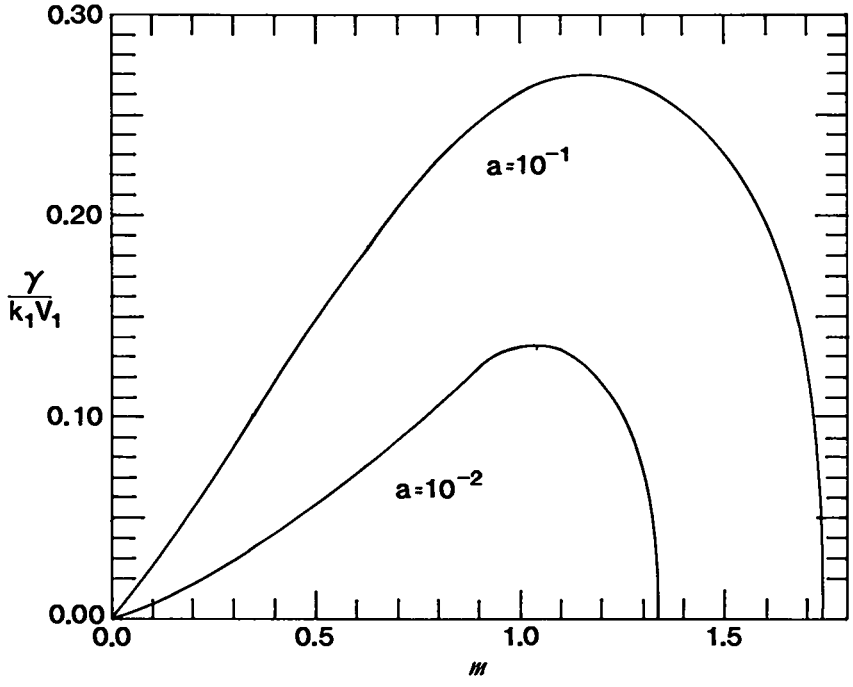

Fig. 4. Unstable growth rates in the generalized Gerwin problem when $\rho_1/\rho_2 = 10^{-1}$, 10^{-2}, and the media are in "pressure equilibrium" ($\rho_1V_1^2 = \rho_2V_2^2$).

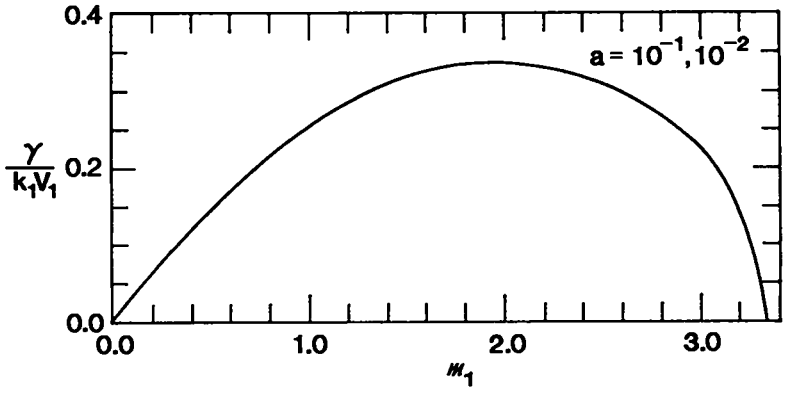

Fig. 5. Unstable growth rates in the generalized Gerwin problem when $\rho_1/\rho_2 = 10^{-1}$, 10^{-2}, and $\rho_1 V_1 = \rho_2 V_2$.

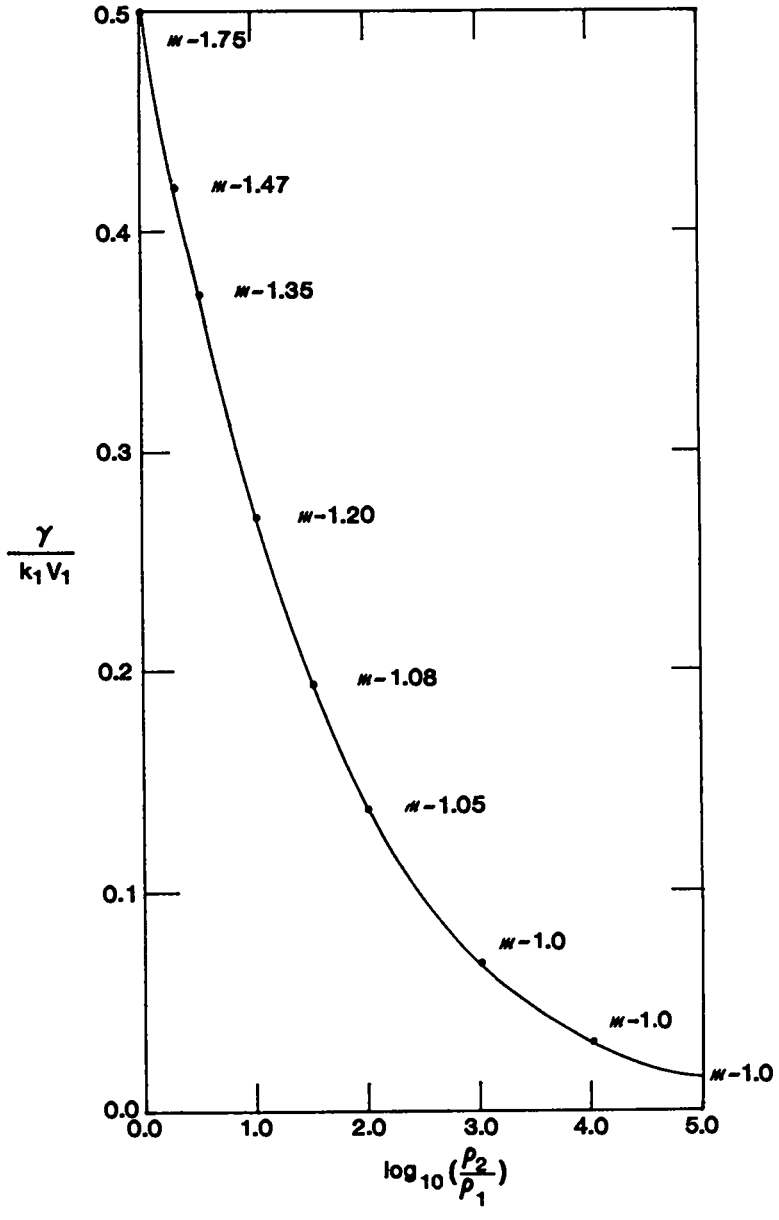

Fig. 6. Maximum unstable growth rates in the generalized Gerwin problem in "pressure equilibrium" as a function of density contrast.

maximum growth rate when $k_1 a \sim 1$, where a is the characteristic thickness of the shear layer. When compressibility is included, MP find that the optimal value of $k_1 a$ decreases with increasing Mach number. In their models, which employed a hyperbolic tangent velocity profile, K-H instabilities can occur only if $m < 2$. (Recall that, for the discontinuous velocity profile, $m < \sqrt{8}$.) As we would expect, the MP growth rates become smaller as m^{-1} diminishes (i.e., as compressibility becomes more important). Unfortunately, in the present context, the MP models do not allow for density stratification. However, a model that includes both velocity shear and density layering is illustrated in Fig. 7.

We will consider only the incompressible case because (1) the growth rates are greatest in that limit and (2) the incompressible problem can be solved exactly and straightforwardly. Although Chandrasekhar[1] does not treat the density layering in enough detail for our application, he does provide an excellent outline of the solution to this problem (p. 487). For all three regions in Fig. 7, the differential equation for w' simplifies to

$$(D^2 - k_1^2)w' = 0 \quad . \tag{26}$$

Therefore, the solutions in the respective regions are

$$w_1' = A\, e^{-k_1 z} \quad , \tag{27a}$$

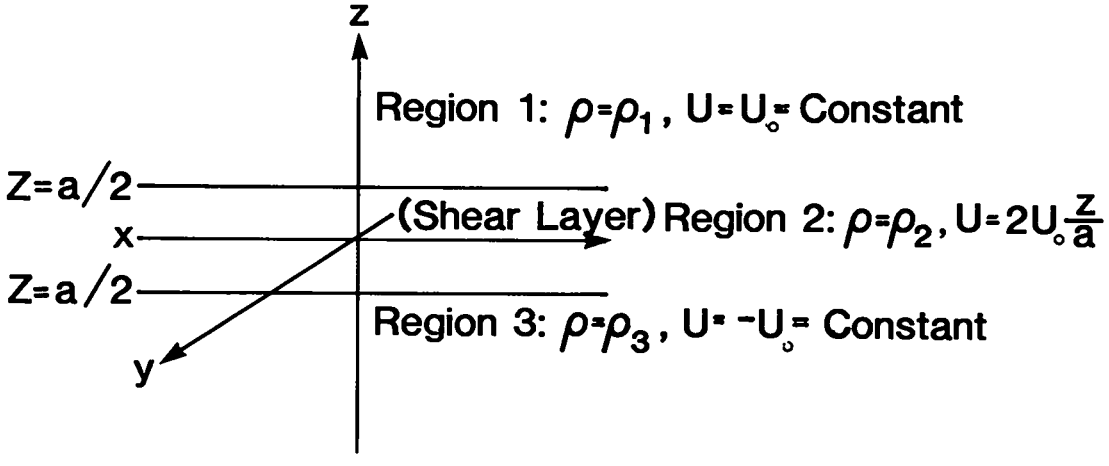

Fig. 7. The three-layer model with linear velocity shear.

$$w_2' = A_o\, e^{-k_1 z} + B_o\, e^{k_1 z} \quad , \tag{27b}$$

and

$$w_3' = B\, e^{k_1 z} \quad , \tag{27c}$$

where A, A_o, B_o, and B are constants. At the interface (i) between regions 1 and 2, the following condition[1] holds:

$$\rho_1(n + k_1U_o)Dw_{1i}' - \rho_2(n + k_1U_o)Dw_{2i}' + 2k_1\rho_2\left(\frac{U_o}{a}\right) w_{2i}' = 0 \quad . \tag{28}$$

Moreover, the displacements must be continuous at the interface;

$$Z_{1i}' = \frac{-i\, w_{1i}'}{(n + k_1U_o)} = Z_{2i}' = \frac{-i\, w_{2i}'}{(n + k_1U_o)} \quad . \tag{29}$$

Consequently, at the interface,

$$w_{1i}' = w_{2i}' \quad . \tag{30}$$

Using Eqs. (27a), (27b), (28), and (30), we obtain

$$\frac{A_o}{B_o}\, e^{-k_1 a} = -\frac{\left[\frac{2U_o}{a} - (n + k_1U_o) - \frac{\rho_1}{\rho_2}(n + k_1U_o)\right]}{\left[\frac{2U_o}{a} + (n + k_1U_o) - \frac{\rho_1}{\rho_2}(n + k_1U_o)\right]} \quad . \tag{31}$$

The interface between regions 2 and 3 may be treated similarly, yielding

$$\frac{B_o}{A_o} e^{-k_1 a} = - \frac{\left[\frac{2U_o}{a} + (n - k_1 U_o) + \frac{\rho_3}{\rho_2}(n - k_1 U_o)\right]}{\left[\frac{2U_o}{a} - (n - k_1 U_o) + \frac{\rho_3}{\rho_2}(n - k_1 U_o)\right]} \quad . \tag{32}$$

We define the following dimensionless quantities: $r_1 = \rho_1/\rho_2$, $r_3 = \rho_3/\rho_2$, $\kappa = k_1 a$, and $y = n/k_1 U_o$. In these variables, Equations (31) and (32) may be combined to form the quadratic equation

$$\left[(1 + r_1)(1 + r_3) - (1 - r_1)(1 - r_3)e^{-2\kappa}\right]y^2 - \frac{2}{\kappa}(r_3 - r_1)(1 - e^{-2\kappa})y$$

$$-\left[\left(\frac{2}{\kappa} - 1 - r_1\right)\left(\frac{2}{\kappa} - 1 - r_3\right) - \left(\frac{2}{\kappa} + 1 - r_1\right)\left(\frac{2}{\kappa} + 1 - r_3\right)e^{-2\kappa}\right] = 0 \quad . \tag{33}$$

For the uniform medium ($r_1 = r_2 = 1$),

$$y = \pm\kappa^{-1}\left[(\kappa - 1)^2 - e^{-2\kappa}\right]^{1/2} \quad , \tag{34}$$

a result originally due to Rayleigh (see reference 1). In this case, if instabilities exist they contain no oscillatory component in the calculational frame. Instabilities exist if $e^{-2\kappa} > (\kappa - 1)$, implying that $\kappa < \kappa_c = 1.278465$.

In order to demonstrate the connection between this three-layer problem and the incompressible, discontinuous case, we let $\kappa \to 0$ in Equation (33), meaning that the shear layer is arbitrarily thin in comparison with the perturbation wavelength. The resulting equation is

$$y^2 - 2\frac{(r_3 - r_1)}{(r_3 + r_1)} + 1 = 0 \quad . \tag{35}$$

Letting $r_1 = r_3^{-1}$, Equation (35) may be rewritten as

$$y^2 - 2(1 - 2\alpha) + 1 = 0 \quad , \tag{36}$$

where

$$\alpha = \rho_1/(\rho_1 + \rho_3) \quad .$$

Hence,

$$y = (1 - 2\alpha) \pm 2i\alpha^{1/2}\sqrt{(1 - \alpha)} \quad . \tag{37}$$

With respect to a rest frame in medium 3 (the fireball),

$$n = -\alpha k_1 U \pm i\sqrt{\alpha(1 - \alpha)}\, k_1 U \quad , \tag{38}$$

where $U = U_1 - U_3 = 2U_o$. This expression is identical with Eq. (24), the complex growth rate for an incompressible fluid with velocity discontinuity U.

The growth rates for the constant density case with linear velocity shear are shown in Fig. 8. The quantity $y_I(\kappa)$ is the magnitude of the imaginary part of dimensionless angular frequency y. Also shown in Fig. 8 is the more conventional, normalized growth rate,[2] $\gamma a/U = y(\kappa)\kappa/2$. Our solutions for this quantity are close to the MP solutions for the hyperbolic tangent velocity profile (shown in their Fig. 3). Graphs of $\gamma a/U$ for four different representative models are shown in Figs. 9-12. The dashed lines on these figures show the incompressible, discontinuous growth rates. As was the case with our previous models, the growth rates diminish rapidly with increasing density contrast. Also, the wavenumber at which the growth is most rapid decreases slowly with increasing density contrast. Figure 13 depicts the maximum growth rate, as well as the corresponding values of κ, as a function of total density contrast, ρ_3/ρ_1, for models having $\rho_1/\rho_2 = \rho_2/\rho_3$. With respect to a rest frame in region 3, the frequencies of oscillation are comparable to their corresponding maximum growth rates.

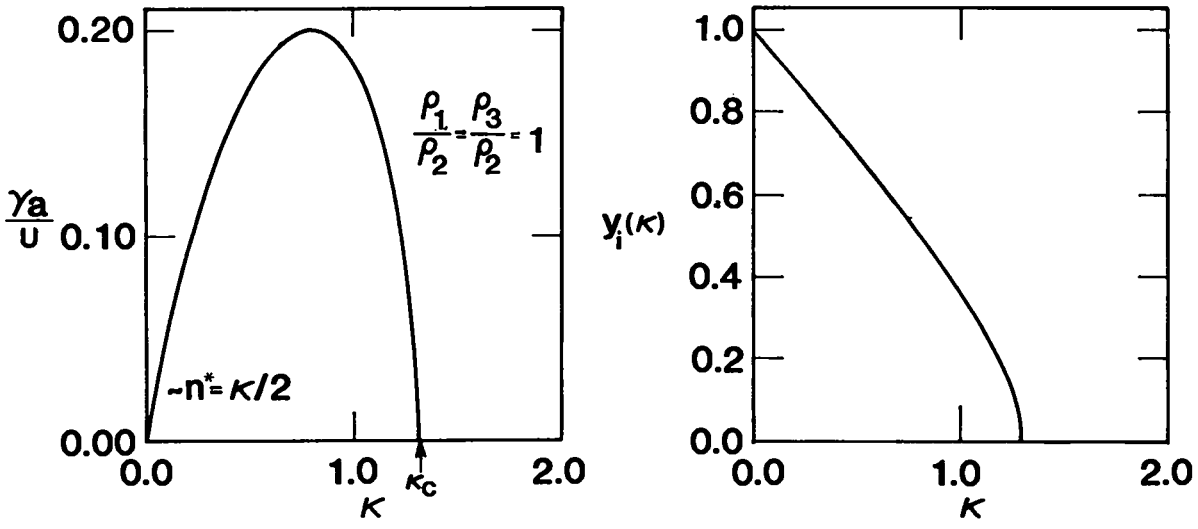

Fig. 8. Unstable growth rates in the three-layer problem when $r_1 = r_3 = 1$.

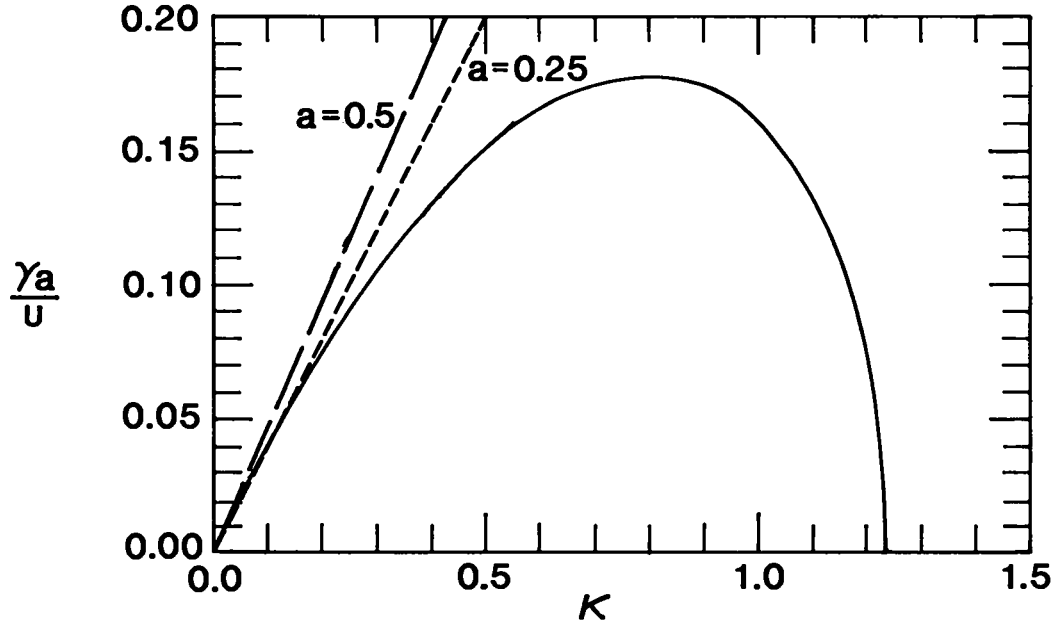

Fig. 9. Unstable growth rates in the three-layer problem when $r_1 = 1/2$ and $r_3 = 2$.

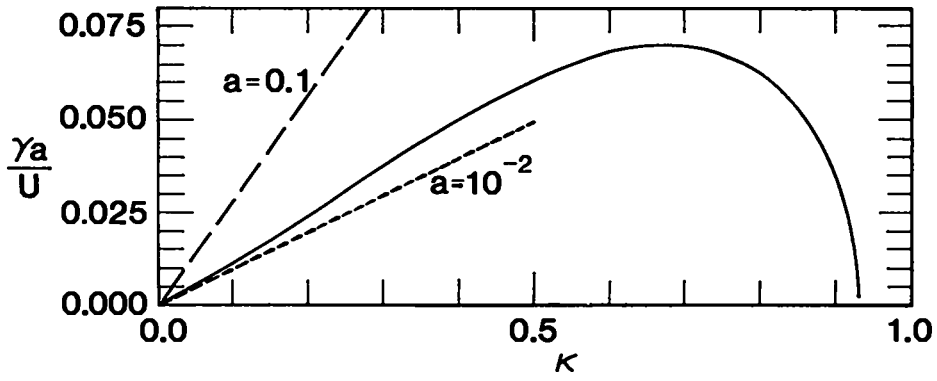

Fig. 10. Unstable growth rates in the three-layer problem when $r_1 = 10^{-1}$ and $r_3 = 10$.

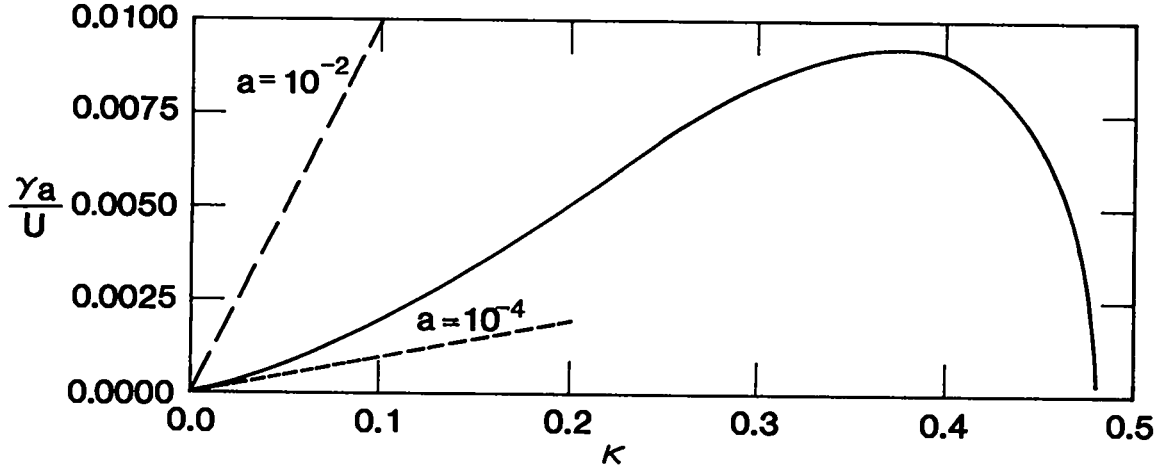

Fig. 11. Unstable growth rates in the three-layer problem when $r_1 = 10^{-2}$ and $r_3 = 100$.

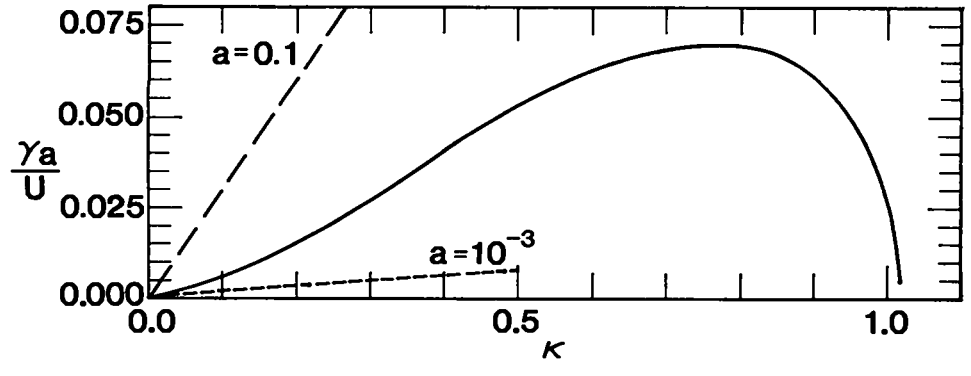

Fig. 12. Unstable growth rates in the three-layer problem when $r_1 = 10^{-3}$ and $r_3 = 10$.

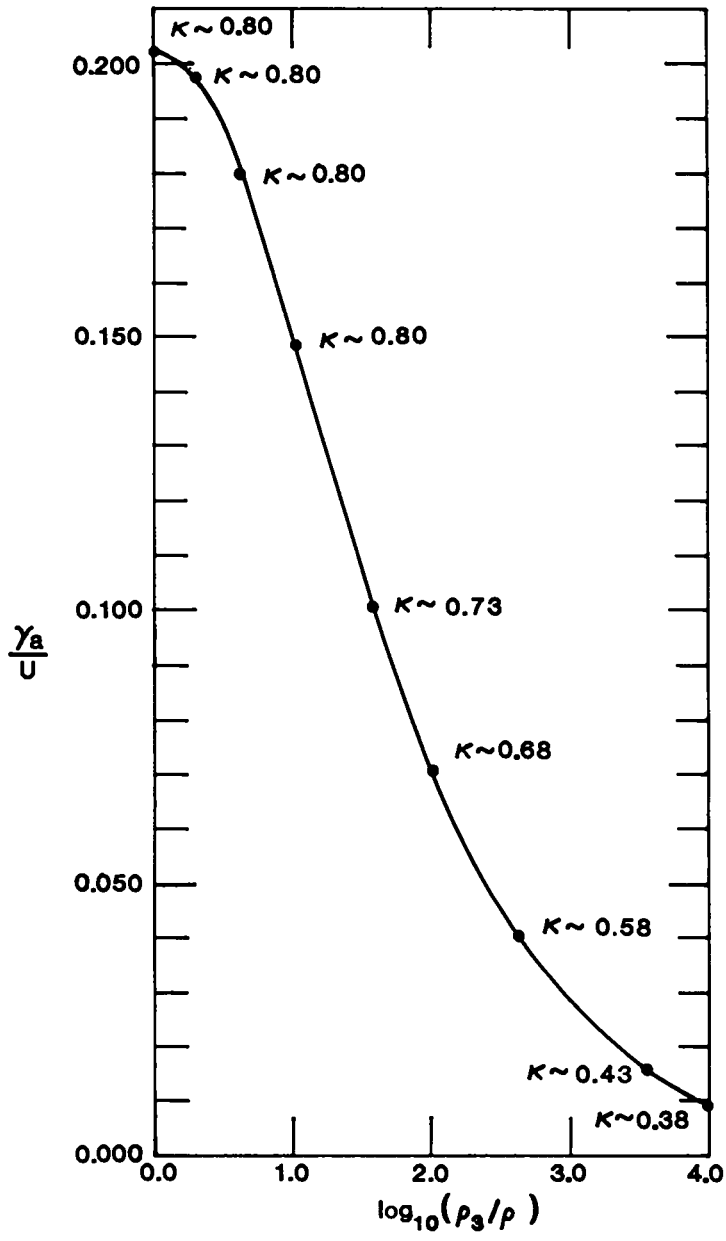

Fig. 13. Maximum unstable growth rates in the three-layer problem as a function of ρ_3/ρ_1 when $\rho_1/\rho_2 = \rho_2/\rho_3$.

REFERENCES

1. S. Chandrasekhar, Hydrodynamic and Hydromagnetic Stability, Sections 100, 101, 102, and 106 (Dover Publications, Inc., New York, 1981).

2. A. Miura and P. L. Pritchett, "Nonlocal Stability Analysis of the MHD Kelvin-Helmholtz Instability in a Compressible Plasma," J. Geophys. Res. 87, 7431 (1982).

3. R. A. Gerwin, "Stability of the Interface Between Two Fluids in Relative Motion," Rev. Mod. Phys. 40, 652 (1968).

Printed in the United States of America
Available from
National Technical Information Service
US Department of Commerce
5285 Port Royal Road
Springfield, VA 22161

Microfiche (A01)

Page Range	NTIS Price Code	Page Range	NTIS Price Code	Page Range	NTIS Price Code	Page Range	NTIS Price Code
001-025	A02	151-175	A08	301-325	A14	451-475	A20
026-050	A03	176-200	A09	326-350	A15	476-500	A21
051-075	A04	201-225	A10	351-375	A16	501-525	A22
076-100	A05	226-250	A11	376-400	A17	526-550	A23
101-125	A06	251-275	A12	401-425	A18	551-575	A24
126-150	A07	276-300	A13	426-450	A19	576-600	A25
						601-up*	A99

*Contact NTIS for a price quote.

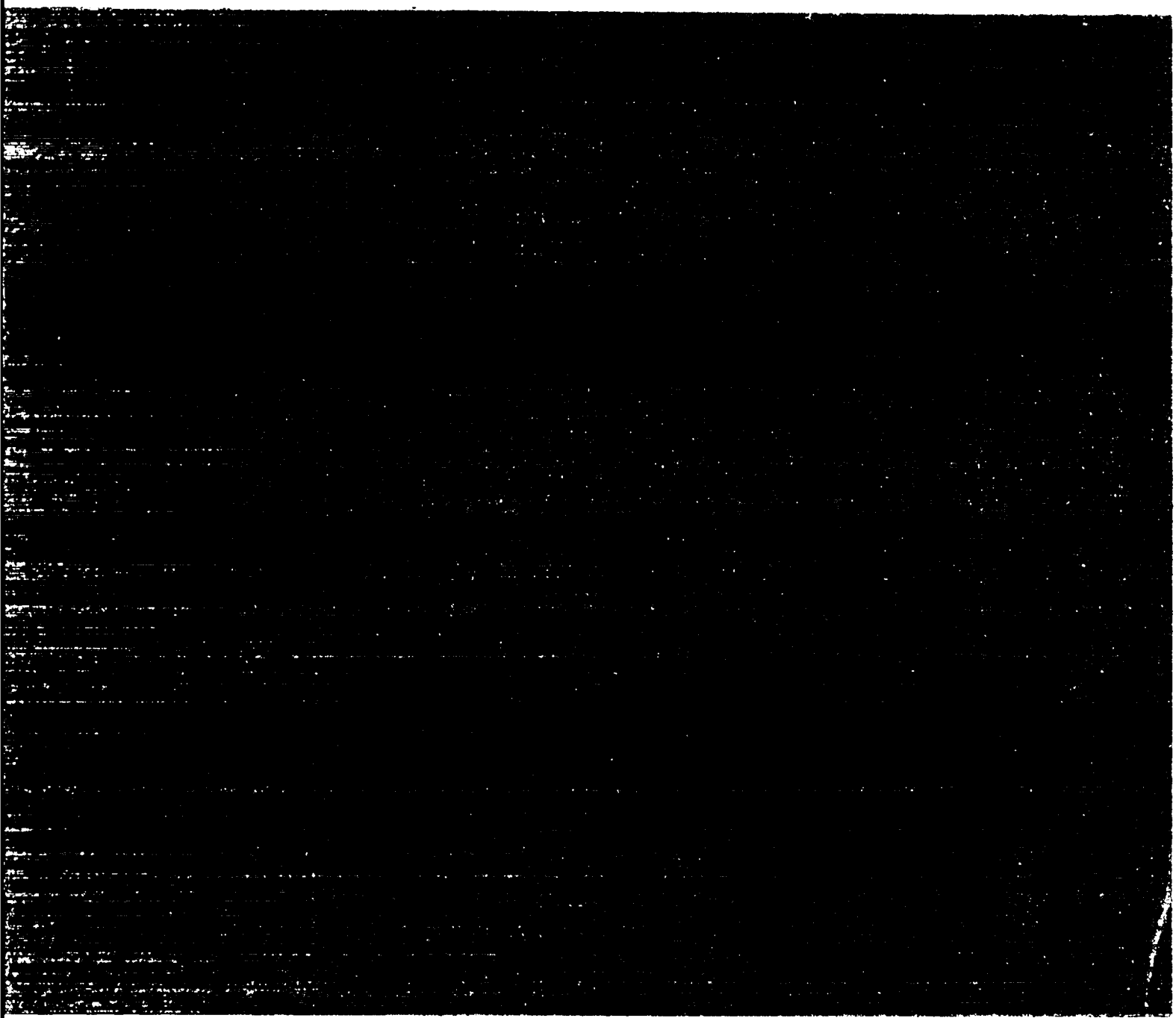

Los Alamos